PHYSICAL REVIEW B

CONDENSED MATTER

THIRD SERIES, VOLUME 49, NUMBER 12 15 MARCH 1994-II

Solid-state effects and atomiclike effects on shallow inner-shell-electron energy-loss spectra of a cation p or d hole in sulfides

Youichi Ohno

Department of Physics, Faculty of General Education, Utsunomiya University, 350 Mine-machi, Utsunomiya 321, Tochigi, Japan

(Received 4 August 1993; revised manuscript received 24 November 1993)

Inner-shell-electron energy-loss spectroscopy studies have been done for the systems in which a shallow p or d core hole exists in the final state of a cation. Optically allowed and forbidden transitions have been distinguished from spectral variations due to the breakdown of dipole selection rules. The Ti and V $M_{2,3}$ spectra and the Zr, Nb, and Mo $M_{4,5}$ spectra in layered transition-metal disulfides and related misfit-layer compounds are well explained in terms of the energy-band structures. The overall structures of the Pb and Bi $O_{4,5}$ spectra are understood within the atomic model containing j-j coupling. The Sn $N_{4,5}$ spectra in SnS and SnS_2 are intermediate between them. A reasonable explanation is given by both the atomic model and the band-structure model.

I. INTRODUCTION

A core hole in x-ray-absorption spectroscopy (XAS), inner-shell-electron energy-loss spectroscopy (ISEELS), and x-ray photoelectron spectroscopy (XPS) interacts to a greater or lesser degree with valence electrons by an attractive Coulomb potential and often gives rise to excitoniclike structures and satellite peaks. Since the Coulomb potential in rare-earth compounds and ionic transition-metal compounds is poorly screened, their spectra reveal multiplet structures arising from exchange and Coulomb interaction between a core hole and localized valence f or d electrons.[1-3] They often reveal satellite peaks which arise from interconfiguration interaction between poorly and well screened final states.[4-6] This interaction is particularly important in systems with strong hybridization with surrounding atoms, because the screening occurs by charge transfer from ligands. If the transferred electrons occupy empty states that are shifted downward in energy below the Fermi level by the Coulomb potential, the relaxation process is termed the shakedown process. If they occupy empty states above the Fermi level, the process is termed the shakeup process. Thus the Coulomb interaction and the hybridization are key factors characterizing core-electron spectra. Here it is worth noting that core-hole effects are generally smaller in XAS and ISEELS than in XPS because an excited electron from a core level is utilized for the screening.

Zaanen *et al.*[7] have indicated that the exchange interaction coupled with the spin-orbit interaction brings about a large deviation from the statistical-intensity ratio of the $L_{2,3}$ peaks of light transition metals. In calculations, they have used multipole Coulomb and exchange terms of about 80% of the atomic values to give a reasonable agreement between theory and experiment. Although the Coulomb and exchange interactions are stronger in XPS, the spectra give the statistical intensity ratio to the $2p_{3/2}$ and $2p_{1/2}$ peaks. This strange result is caused by the matrix-element effect. Since the transitions in XAS obey dipole selection rules, the intensities and the shape are affected by matrix elements in the transition probability. Such an effect is not present in XPS. Thus the matrix-element effect involving spins is another key factor characterizing XAS and ISEELS spectra. Thole and van der Laan[8] have studied the spectral variations under coupling conditions intermediate between the LS and j-j limits for the $3d$ transition metals.

Since the final states are the same in both XAS and ISEELS and the transitions obey dipole selection rules at high incident energy in spite of different excitation probes, that is, photons in XAS and electrons in ISEELS, their spectra resemble each other. However, ISEELS spectra at low incident energy allow optically forbidden transitions due to the breakdown of the dipole selection rules. As the incident energy E_0 decreases, momentum transfer $\mathbf{q}$ $(=\mathbf{k}_0-\mathbf{k}')$ rapidly increases (where $\mathbf{k}_0$ and $\mathbf{k}'$ are the wave vectors of an incident electron and an inelastically scattered electron). A large momentum transfer enables quadrupole and multipole transitions as well as dipole transitions. At small E_0 optically forbidden transitions are also allowed by exchange interaction between a slow incident electron and an excited electron.[9] This interaction relaxes the conditions for the spin

0163-1829/94/49(12)/7851(10)/$06.00

angular momentum $S=0$ as well as the orbital angular momentum $L=0,1$ and the total angular momentum $J=0,1$. Then we may regard ISEELS at small E_0 as intermediate between XAS and XPS; the final states are the same as those in XAS and the transitions do not obey dipole selection rules, like XPS transitions.

This paper presents the ISEELS spectra of shallow p or d core holes in the transition metals, Sn, Pb, and Bi which are contained in layered transition-metal disulfides, the misfit-layer compounds $(MS)_{1+x}TS_2$ (M=Sn,Pb, Bi,Ce,Sm; T=Ti,V,Nb), $PbZrS_3$, and related compounds. In the spectra, the spin-orbit (SO) interaction and the electron-hole (e-h) interaction are comparable to the crystal-field splitting and the dispersion of unoccupied energy states. Thus, both atomic and solid-state effects are important.

The crystal structure of the misfit-layer compounds is isotypic with that of $LaCrS_3$; they are constructed of alternately stacked MS and TS_2 layers.[10] For simplicity they are denoted here by MTS_3. Among them $SnTiS_3$, $PbTiS_3$, and $MNbS_3$ (M=Sn,Pb,Bi,Ce,Sm) have metallic conductivity parallel to the layers, and $PbVS_3$ reveals semiconducting properties. The atomic arrangement of a MS layer resembles that of TII, which is approximated by a rocksaltlike lattice sliced with two parallel planes with an interplanar distance of half the lattice constant. Bulk PbS and SnS are narrow-gap semiconductors with band gaps of 0.29 and 1.1 eV, respectively, and BiS is not found. The atomic arrangement of a TS_2 layer is identical to that of the bulk TS_2 compound. Bulk TiS_2 is a narrow-gap semiconductor and VS_2 and NbS_2 are metallic. The crystal of $PbZrS_3$ consists of columns of double edge-sharing Zr_2S_6 octahedra which are linked by Pb atoms in tricapped trigonal-prismatic coordination.[11] Thus, it is a three-dimensional compound with the NH_4CdCl_3 structure rather than a two-dimensional compound.

II. EXPERIMENTS

ISEELS spectra of Ti $M_{2,3}$ and $L_{2,3}$, V $M_{2,3}$, Zr $N_{2,3}$ and $M_{4,5}$, Nb $N_{2,3}$, Mo $M_{4,5}$, Sn $N_{4,5}$, Pb $O_{4,5}$, and Bi $O_{4,5}$ have been measured in reflection geometry with a double-pass cylindrical-mirror analyzer (PHI model no. 15-255G) equipped with a coaxial normal-incidence electron gun operated in ultrahigh vacuum of 10^{-8} Pa. Since the shallow-peaked core spectra are superimposed on large secondary-electron emission, most of the measurements have been carried out in the second-derivative mode to eliminate the background. In this mode, energy resolution increases with decreasing E_0. Momentum transfer in our system is given by[12]

$$q=\sqrt{2}k_0[(1-\theta_e)-(1-2\theta_e)^{1/2}\cos\theta]^{1/2} \quad (1)$$

and

$$\theta_e=\frac{\Delta E}{2E_0} , \quad (2)$$

where E_0 is the incident energy, ΔE is the energy loss, and θ is the inelastic-scattering angle. In the process, forward-inelastic-scattering events are dominant, accompanied by large elastic scattering. A simple calculation shows that the maximum number of inelastic-scattering events occurs at $\theta=\theta_e$ when $\theta_e \ll 1$. If $\theta_e \ll 1$ and $\theta \ll 1$, Eq. (1) is rewritten as

$$q=k_0(\theta_e^2+\theta^2)^{1/2} . \quad (3)$$

It is then found that q increases with ΔE, but decreases with E_0. The detailed analysis has been made in a previous paper.[13] To investigate the momentum-transfer dependence the spectra have been measured at various E_0.

Single crystals of the layered transition-metal disulfides TS_2 (T=Ti,V,Zr,Mo), the misfit-layer compounds MTS_3 (M=Sn,Pb,Bi,Ce,Sm; T=Ti,V,Nb), and $PbZrS_3$ were prepared by chemical-vapor-transport reaction in a sealed silica ampoule. Atomically clean and smooth surfaces except for $PbZrS_3$ were prepared by cleaving with adhesive tape in the atmosphere just before the measurements. The clean surface of $PbZrS_3$ was prepared by cutting the crystal with a knife edge.

III. RESULTS AND DISCUSSION

A. $L_{2,3}$ and $M_{2,3}$ ISEELS spectra of light 3d transition metals

1. Ti $L_{2,3}$ and $M_{2,3}$ spectra

In a previous paper[13] we have shown that the peak intensities of the Ti $L_{2,3}$, Ti $M_{2,3}$, and S $L_{2,3}$ spectra in TiS_2 and $TiSe_2$ vary from the XAS values as E_0 decreases. At small E_0 the $I(L_3)/I(L_2)$ ratio approaches the statistical value, and the near-edge structures of each branch come to resemble those of the $M_{2,3}$ spectrum. Figure 1 shows the Ti $M_{2,3}$, Ti $L_{2,3}$, S $L_{2,3}$ ISEELS spectra, the S K XAS spectrum, and the calculated density of unoccupied energy states[14] for TiS_2. It is found that there is a strong correlation among them, and the lower-incident-energy spectra resemble the normal-incidence inverse-photoemission spectroscopy (IPS) spectrum[15,16] free from core-hole effects. The k dispersion curves deduced from the IPS spectrum agree with the theoretical results of Zunger and Freeman[17] except for a constant energy displacement. The energy bands have a localized character owing to the quasi-two-dimensional electronic structure, but the experimental results suggest that the e-h interaction is smaller than the crystal-field splitting and the dispersions of the t_{2g} and e_g bands, and that the matrix-element effect is more important for the spectra.

In the present study we investigate the variations arising from the donation of d electrons, because this brings about different behavior for the spectra in the atomic model and the band-structure model. Figure 2 shows the Ti $M_{2,3}$ ISEELS spectra in $SnTiS_3$. In this compound charge transfer occurs from SnS layers to TiS_2 layers and the number of d electrons within a TiS_2 layer is increased by the transferred electrons. The near-edge structures in the range of 32–38 eV are derived from Ti 3d-like states and the structures in the range of 38–44 eV are derived from the 4s- and 4p-like states. The 3d-like states are split into t_{2g} and e_g bands by the crystal field in octahe-

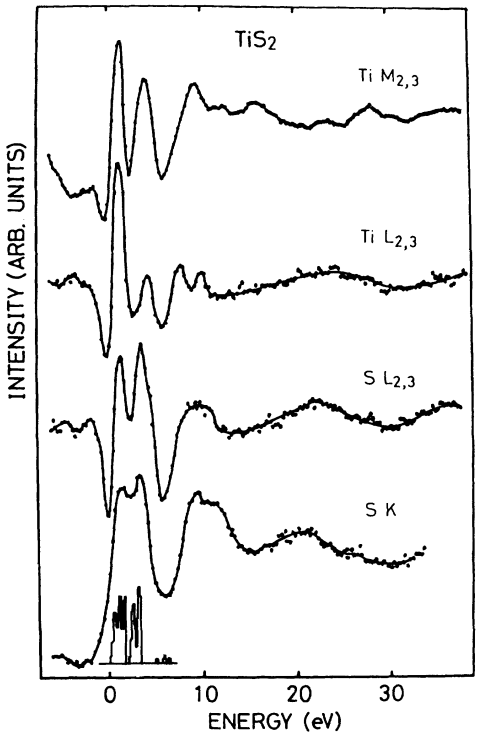

FIG. 1. Ti $M_{2,3}$, Ti $L_{2,3}$, S $L_{2,3}$ ISEELS spectra, S K XAS spectrum, and calculated density of unoccupied energy states (Ref. 14) for TiS_2.

dral coordination. As E_0 decreases, the intensity of the t_{2g} peak increases and a shoulder appears on the lower-energy side of the e_g peak. This shoulder is caused by reduced symmetry due to the change of crystal structure from hexagonal to triclinic. The crystal distortion also splits the t_{2g} levels into the d_{z^2} level and the upper d_{xy} and $d_{x^2-y^2}$ levels, where the z axis is in accord with the c axis perpendicular to the layers. The increased intensity of the t_{2g} peak at small E_0 is caused by the breakdown of dipole selection rules and/or the polarization effect due to large momentum transfer.[13,18] If transferred electrons fill the d_{z^2} band, we may expect reduced intensity or width of the first peak in the band-structure model. A linear combination of atomic orbitals calculation[19] shows that the d_{z^2} band contains the d_{xy} type of orbitals and a d_{z^2}-like character is involved in the upper d_{xy} and $d_{x^2-y^2}$ bands by various $d-d$ hybridizations and lattice periodicity. In the circumstances we may consider that charge transfer to the d_{z^2} band results in a decrease in the peak width without a significant change of intensity. The experimental spectrum shows reduced width. The intensity remains unchanged.

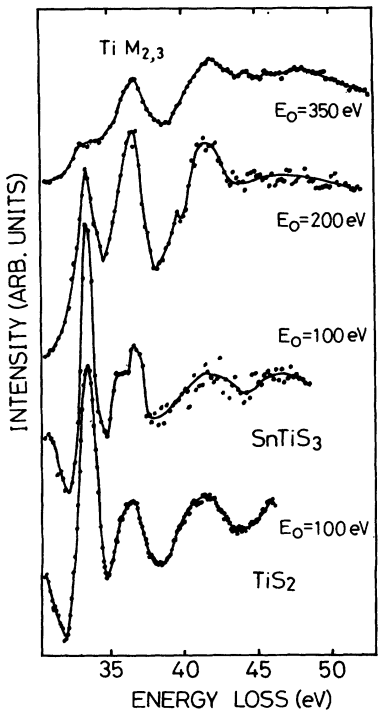

FIG. 2. Ti $M_{2,3}$ ISEELS spectra in $SnTiS_3$ and TiS_2.

In the atomic model, the shoulder on the lower-energy side of the e_g peak can be explained by the change of symmetry from O_h to D_{4h} as discussed by de Groot *et al.*[20] However, no explanations are given for the similarity between the $L_{2,3}$ and $M_{2,3}$ spectra at small E_0, because the e-h interaction gives different transition probabilities and energy distributions of multiplet terms for a shallow $3p$ and a relatively deep $2p$ hole, as confirmed by Yamaguchi *et al.*[21] and Thole and van der Laan.[8] If an electron is transferred from SnS to TiS_2 layers, the $3p^5 3d^2$ final state has a larger number of multiplet terms ($^4G, ^4F, ^4D, ^4P, ^2G, ^2F, ^2D, ^2P$) than the nontransferred final state $3p^5 3d^1$ ($^3F, ^3D, ^3P, ^1F, ^1D, ^1P$). Then we may expect an increase in the width of d-like structures, in contrast to the experimental result.

2. *V $M_{2,3}$ spectra*

The V $M_{2,3}$ ISEELS spectra in $PbVS_3$ at $E_0 = 130$, 200, and 350 eV are shown in Fig. 3. Since the compound is akin to $SnTiS_3$ and V is surrounded by six S atoms in a distorted octahedron,[22] the spectra show structures similar to those of $SnTiS_3$, excluding the reduced t_{2g} peak. Since a V atom has one more $3d$ electron than a Ti atom, the d_{z^2} band is filled with additional d electrons. Then the experimental result is explained satisfactorily in terms of the rigid-band model. On the other hand, the atomic model does not seem valid. Recently, de Groot *et al.*[23] have calculated Ti and V $L_{2,3}$ XAS spectra based on the atomic model. Both spectra depend strongly on the $10Dq$ value. Although they reveal relatively similar structures at about 2 eV, which is a reasonable $10Dq$ value for the compounds, we find many pre-edge structures arising from optically forbidden multiplet terms and a higher intensity of the first main peak relative to the second peak, in contrast to the experimental result.

Figure 4 shows the V $M_{2,3}$ spectra in the V intercalation derivative of VS_2, in which intercalate V atoms occupy half of the octahedral sites within van der Waals gaps. If they are ionized as a tetravalent ion, the t_{2g} band of the host material is half filled with two transferred electrons and one conduction electron per chemical formula. Then

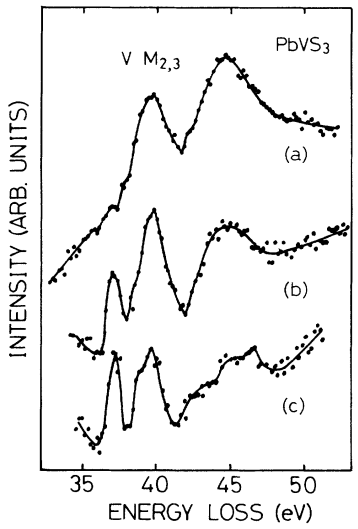

FIG. 3. V $M_{2,3}$ ISEELS spectra in $PbVS_3$: (a) $E_0=350$ eV; (b) $E_0=200$ eV; (c) $E_0=130$ eV.

we may expect further reduced intensity and width. In practice the intensity decreases without large changes of e_g structures and higher-energy structures. Also we find in Fig. 4 that there is a good coincidence between the ISEELS spectrum and the IPS spectrum of VSe_2 (Ref. 24) except for the intensity of the t_{2g} peak. The results may suggest that the rigid-band model is valid for these spectra to the first approximation.

Summarizing the above results we may conclude that the Ti and V $L_{2,3}$ and $M_{2,3}$ spectra in TS_2 and MTS_3 (T=Ti,V) are well explained in terms of the energy-band structures rather than the atomic model.

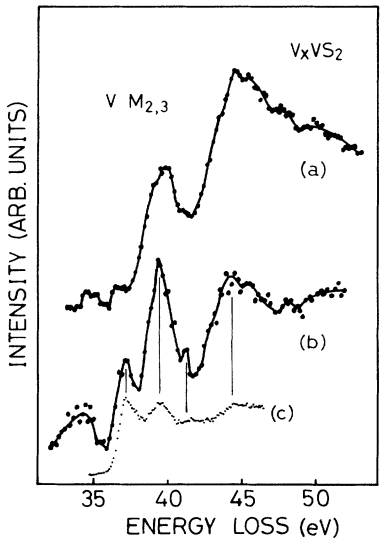

FIG. 4. V $M_{2,3}$ ISEELS spectra in V_xVS_2 ($x=0.5$): (a) $E_0=350$ eV; (b) $E_0=200$ eV. (c) Normal-incidence inverse-photoemission spectrum of VSe_2 at $h\nu=26$ eV (Ref. 24).

B. $M_{4,5}$ and $N_{2,3}$ ISEELS spectra of the 4d transition metals

In this section we discuss the Zr, Nb, and Mo $M_{4,5}$ and $N_{2,3}$ ISEELS spectra in compounds belonging to the same family as TiS_2. Since the oscillator strength for $d-f$ channels is very small due to a large centrifugal barrier, $d-p$ transitions are dominant near the threshold at $q=0$. Since optically forbidden $d-d$ transitions are allowed at $q\neq 0$, d-like structures would be observed more prominently at small E_0. Figure 5 shows the Zr $M_{4,5}$ ISEELS spectra in ZrS_2 and $PbZrS_3$, which contain the S $L_{2,3}$ loss structures on the lower-energy side. In spite of different crystal structures, both spectra are quite similar except for the peak intensities of the S $L_{2,3}$ structures. The higher intensities in $PbZrS_3$ are due to a higher concentration of S atoms. Both Zr atoms are in similar local atomic environments, having the same average Zr-S distance of about 2.5 Å. Thus, the similarity arises from the local nature of core-electron spectra. For comparison, the Zr $M_{4,5}$, Zr $N_{2,3}$, and S $L_{2,3}$ ISEELS spectra in $PbZrS_3$ are shown in Fig. 6, together with the S K XAS spectrum and the density of unoccupied energy states calculated for ZrS_2.[14] Although the S K and S $L_{2,3}$ spectra include an additional contribution from S atoms in tricapped trigonal prisms, there is good agreement among the spectra and the density of states, indicating that the near-edge structures represent unoccupied energy states in the neighborhood of excited atoms. The first and second peaks are assigned to the t_{2g} and e_g bands and the third peak to the metal sp bands.

The small SO splitting of Zr 3d levels results in overlaps between the t_{2g} peak in the M_4 branch and the e_g peak in the M_5 branch, and between the e_g peak in the M_4 branch and the metal sp peak in the M_5 branch. This is shown clearly in Fig. 7, in which the Zr $M_{4,5}$ spectrum in $PbZrS_3$, the Mo $M_{4,5}$ spectrum in MoS_2, and the Nb $N_{2,3}$ spectrum in $CeNbS_3$ are compared, aligned at the peak position of the metal sp bands. Since the Mo and Nb atoms are surrounded by six S atoms in a trigonal

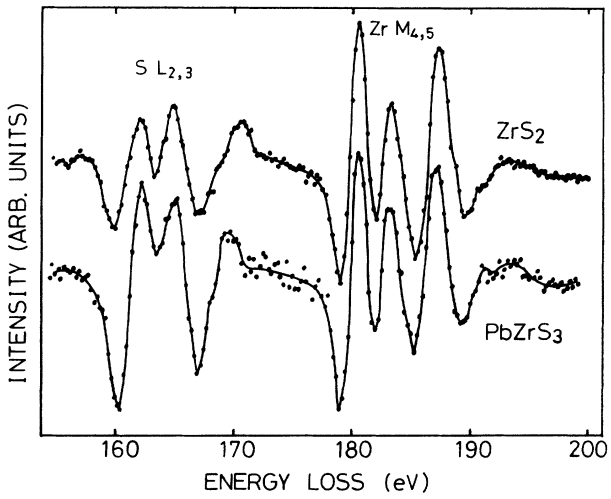

FIG. 5. Zr $M_{4,5}$ and S $L_{2,3}$ ISEELS spectra in ZrS_2 and $PbZrS_3$. They have been measured at $E_0=500$ eV.

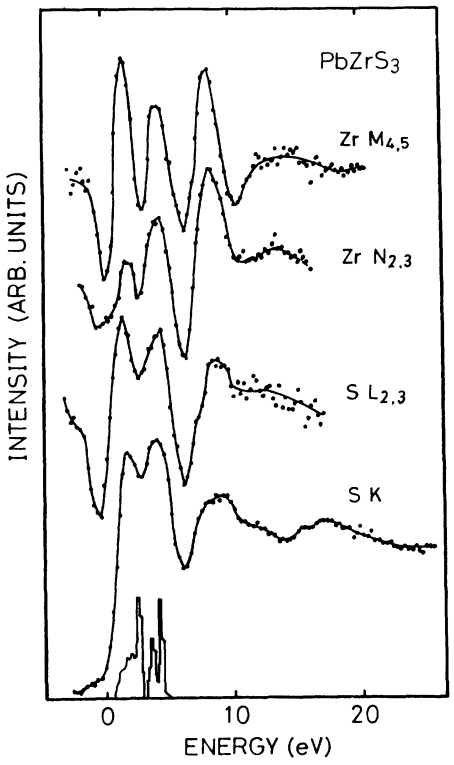

FIG. 6. Comparison among the Zr $M_{4,5}$, Zr $N_{2,3}$, and S $L_{2,3}$ ISEELS spectra and the S K XAS spectrum in $PbZrS_3$ and the calculated density of conduction-band states of ZrS_2 (Ref. 14).

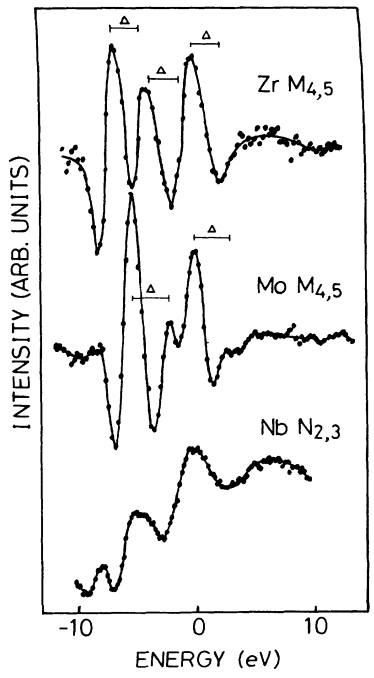

FIG. 7. Comparison among the Zr $M_{4,5}$ ISEELS spectrum in $PbZrS_3$, the Mo $M_{4,5}$ ISEELS spectrum in MoS_2, and the Nb $N_{2,3}$ ISEELS spectrum in $CeNbS_3$. Δ denotes the spin-orbit splitting of core 3d levels, which is 2.5 and 3.0 eV for Zr and Mo, respectively. The origin of the horizontal axis is the peak position of the metal sp peak.

prism, the 4d levels are split into d_{z^2}, $d_{x^2-y^2}$, and d_{xy}, and d_{xz} and d_{yz} levels. Since the d_{z^2} band of MoS_2 is completely filled with two d electrons per chemical formula, the peak vanishes in the Mo $M_{4,5}$ spectrum. $CeNbS_3$ has more than one, but less than two d electrons per chemical formula as confirmed by its metallic properties.[25] Then the Nb $N_{2,3}$ spectrum exhibits a small peak corresponding to unoccupied d_{z^2} states near the threshold. This peak is found for all the misfit-layer compounds containing NbS_2 layers, although the intensity depends on the number of d electrons.[26]

Finally, it is worth noting that there is good agreement among the Nb $N_{2,3}$ ISEELS spectra, the Se M_5 XAS spectrum in $NbSe_2$,[27] and the calculated density of states of NbS_2.[19] Also there is agreement among the Mo $M_{4,5}$ ISEELS spectrum, the Mo L_3 and S K XAS spectra[28] the IPS spectrum,[29] and the calculated density of states[14] for MoS_2. The incident-energy dependence of the Mo $M_{4,5}$ spectrum is shown in Fig. 8. The optically forbidden d-like peak near the threshold increases in intensity with decreasing E_0 due to the breakdown of the dipole selection rules. The $I(M_5)/I(M_4)$ ratio is larger than the statistical value at small E_0. These facts imply that the matrix-element effect plays an important role in the spectra. Summarizing the results, we may conclude that the Zr, Nb, and Mo $M_{4,5}$ and $N_{2,3}$ spectra in $PbZrS_3$, TS_2, and MTS_3 (T=Zr,Nb,Mo) are well explained in terms of energy-band structures and the matrix-element effect.

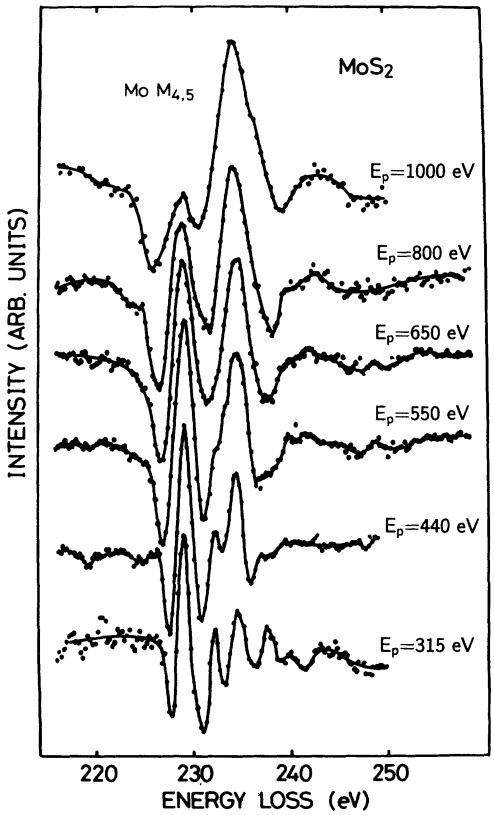

FIG. 8. Mo $M_{4,5}$ ISEELS spectra in MoS_2 at various incident energies.

C. Pb and Bi $O_{4,5}$ ISEELS spectra

1. Peak assignment and j-j coupling

In this section we discuss the $O_{4,5}$ ISEELS spectra of heavy atoms in a solid. Pb and Bi atoms have the large atomic numbers 82 and 83, respectively. In such heavy atoms the j-j coupling or the SO interaction is more important than the LS coupling. The outermost electron configurations of neutral Pb and Bi atoms are $6s^2 6p^2$ and $6s^2 6p^3$, respectively. Then we may expect that the lowest conduction bands of the sulfides consist mainly of metal $6p$ states, and the $O_{4,5}$ spectra reveal a large peak near the threshold due to optically allowed d-p transitions. However, the experimental spectra at large E_0 and the reflectivity spectra reveal only a small peak. A large peak appears at 4 eV above the threshold. As E_0 decreases, the small peak rapidly increases. As shown in Figs. 9 and 10, the intensity is comparable with the large peak at small E_0 and the near-edge structures consist of four peaks marked a, b, c, and d in Fig. 9. The energy values are tabulated in Table I together with the peak energies of the Pb $O_{4,5}$ ISEELS spectra in PbS and PbSe,[30] the reflectivity spectrum in PbSe,[31] and the total secondary-electron yield (TSEY) spectrum in PbS.[32] It is found that the spectra are quite similar in spite of different crystal structures and different local atomic arrangements. The energy separations between the peaks a and b and between a and c are about 1.4 and 3.0 eV, respectively, in close agreement with the separations between c and d and between b and d. This fact implies that the peaks a and b and the peaks c and d show a pair of structures in the O_5 and O_4 branches. The schematic diagram for excitation of $5d$ electrons to unoccupied $6p$ levels is shown in Fig. 11. Among four possible channels the minimum-excitation-energy channel is the optically forbidden $5d_{5/2} \rightarrow 6p_{1/2}$ transitions. This assignment is consistent with the incident-energy dependence of the peak a. At large E_0 it has a small intensity due to the dipole selection rules. The peak around 4 eV above the threshold should be assigned to the $5d_{3/2} \rightarrow 6p_{1/2}$ transitions rather than the $5d_{5/2} \rightarrow 6p_{3/2}$ transitions. This assignment is different from that of Cardona *et al.*,[30] who have attributed it from a simple calculation to the $5d_{5/2} \rightarrow 6p_{3/2}$ transitions. In our assignment the estimated SO splittings for the $6p$ and $5d$ levels are 1.4 and 3.0 eV, respectively. Finally, the peaks b and d are assigned to the optically allowed $5d_{5/2} \rightarrow 6p_{3/2}$ and $5d_{3/2} \rightarrow 6p_{3/2}$ transitions. For the $5d_{3/2} \rightarrow 6p_{3/2}$ transitions, Cardona *et al.* have found that the oscillator strength is 10 times smaller than those of the other optically allowed transitions.

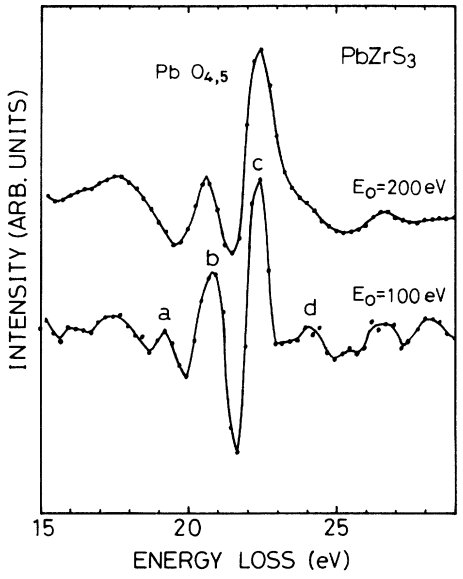

FIG. 9. Pb $O_{4,5}$ ISEELS spectra in $PbZrS_3$ at $E_0 = 100$ and 200 eV. Notations in the figure are explained in the text.

2. Matrix-element effects

Figure 12 shows the Pb $5d$ XPS spectra in $PbNbS_3$ and $PbVS_3$. They reveal only two defined SO-slit peaks. The intensity ratio of the $5d_{5/2}$ peak to the $5d_{3/2}$ peak is slightly smaller than the statistical value. This is due to an overlap of the peaks. In fact, the higher-energy-resolution spectrum of McFeely *et al.*[33] gives the statistical value. In contrast, the $I(O_5)/I(O_4)$ intensity ratio in the reflectivity and ISEELS spectra at large E_0 is quite different from the statistical value. This is due to the matrix-element effect. Cardona *et al.*[30] have discussed the different behaviors of the Pb $O_{4,5}$ spectra in lead chalcogenides and the In $N_{4,5}$ spectrum in InAs, one of the III-V compound semiconductors, in relation to the SO

TABLE I. Energies in eV of the main features of the Pb $O_{4,5}$ ISEELS, reflectivity, and TSEY spectra in $PbMS_3$ (M = Zr,Nb,V), PbS, and PbSe. The ISEELS spectra in PbS and PbSe have been obtained by transmission measurements. The notations a, b, c, and d are shown in Fig. 9.

Notation	$PbZrS_3$ ISEELS	$PbNbS_3$ ISEELS	$PbVS_3$ ISEELS	PbS ISEELS[a]	PbS TSEY[b]	PbSe ISEELS[a]	Reflectivity[c]
a	19.2	19.1	19.0		19.0		19.0
b	20.7	20.5	20.3	19.9	20.0	20.2	20.2
c	22.4	22.1	22.0	22.1	22.0	21.9	21.8
d	24.0	24.0	23.6		23.8	22.8	23.0

[a]Cardona *et al.* (Ref. 30).
[b]Santoni *et al.* (Ref. 32).
[c]Martinez, Schlüter, and Cohen (Ref. 31).

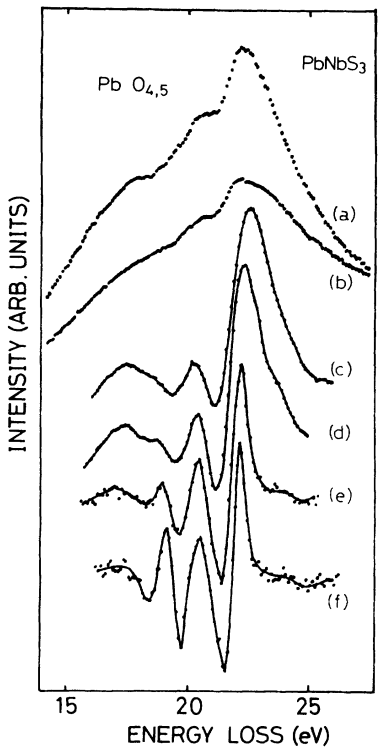

FIG. 10. Pb $O_{4,5}$ ISEELS spectra in $PbNbS_3$ at various incident energies: (a) $E_0=1000$ eV; (b) $E_0=500$ eV; (c) $E_0=350$ eV; (d) $E_0=200$ eV; (e) $E_0=100$ eV; (f) $E_0=70$ eV. The spectra of (a) and (b) have been measured in the pulse-counting mode. The others have been measured in the voltage-modulation mode, which are given in the second-derivative form.

splitting of the outermost p levels. In contrast to the former spectra, the latter shows two similar bands having the relative weights 3 and 2. In InAs, In $5s$ and $5p$ states are strongly hybridized with As $4s$ and $4p$ states, and the SO splitting of the outermost $5p$ levels is small, about 0.4 eV. Then spin compositions are not important for the spectrum. If the SO splitting is small, the transition probability depends only on the orbital angular momenta of the final states, and the spectrum represents the partial

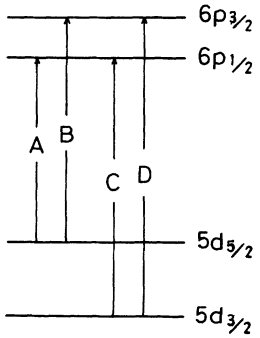

FIG. 11. Schematic diagram for excitation of $5d$ electrons to $6p$ levels. Notation A represents optically forbidden $5d_{5/2}\rightarrow 6p_{1/2}$ transitions which have a minimum excitation energy. Spin-orbit splittings of Pb $5d$ and $6p$ levels which have been evaluated from our ISEELS experiment, are 3.0 and 1.4 eV, respectively.

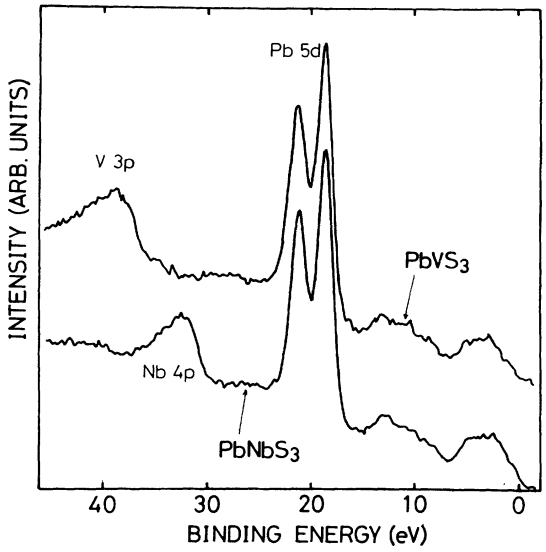

FIG. 12. Pb $5d$ XPS spectra in $PbVS_3$ and $PbNbS_3$ which have been measured with Mg $K\alpha$ radiation.

density of states of particular orbital momenta. However, if the SO splitting is large enough, the transition probability depends on the spin angular momenta as well as the orbital angular momenta. Lead chalcogenides are in the latter case. The theoretical analysis of Santoni *et al.*[32] shows the states with a $6p_{1/2}$ character nine times larger than a $6p_{3/2}$ state at the conduction-band minimum (L point). The calculation of Kohn *et al.*[34] shows SO splitting of about 2 eV at the Γ point. In Fig. 13 the Pb $O_{4,5}$ ISEELS spectrum in $PbVS_3$, the TSEY spectrum in PbS measured by Santoni *et al.*,[32] and the

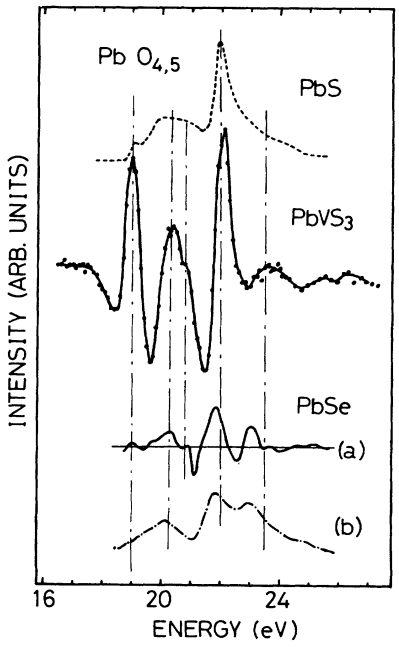

FIG. 13. Comparison among the Pb $O_{4,5}$ ISEELS spectrum in $PbVS_3$, the total secondary-electron yield spectrum in PbS (Ref. 32), and the reflectivity spectrum in PbSe (Ref. 31): (a) second-derivative spectrum of measured reflectivity (b).

reflectivity spectrum in PbSe measured by Martinez, Schlüter, and Cohen[32] are compared. Although the SO splittings of the 5*d* and 6*p* levels is slightly smaller for the selenide than for the sulfides, there is a good coincidence among the spectra. The higher intensity of the first peak in the ISEELS spectrum is due to the breakdown of dipole selection rules. These facts may support the idea that the spectra are explained within the atomic model in the *j-j* coupling limit, and that the matrix-element effect involving the spins is important for the spectra.

The Bi $O_{4,5}$ ISEELS spectrum in $BiNbS_3$ is also quite similar to the Pb $O_{4,5}$ spectra, except for larger width of the first and the third peaks. In Fig. 14 the spectrum is compared with the Pb $O_{4,5}$ ISEELS spectra in $PbVS_3$ and $PbNbS_3$ and the Bi $O_{4,5}$ reflectivity spectrum in BiI_3.[35] The absolute energy of the first peak is 24.8 eV, in agreement with the core binding energy of Bi $5d_{5/2}$ levels estimated by Kowalczyk *et al.*[36] and Margaritondo and Rowe.[37] The intensity decreases with E_0 as observed in the Pb $O_{4,5}$ spectra. Here we may suggest that a peak corresponding to the $5d_{5/2} \rightarrow 6p_{1/2}$ transitions disappears in the reflectivity spectrum in BiI_3 due to dipole selection rules. The lowest-energy peak of the reflectivity spectrum should be connected to the second peak of the ISEELS spectrum, because the absolute energies are nearly equal. The fourth peak, which is ascribed to the $5d_{3/2} \rightarrow 6p_{3/2}$ transitions, is more prominent in the reflectivity spectrum. The main differences in the ISEELS spectrum and the reflectivity spectrum are explained in terms of the matrix-element effect involving the spins of the outermost 6*p* levels, although the band effect might be incompletely ignored.

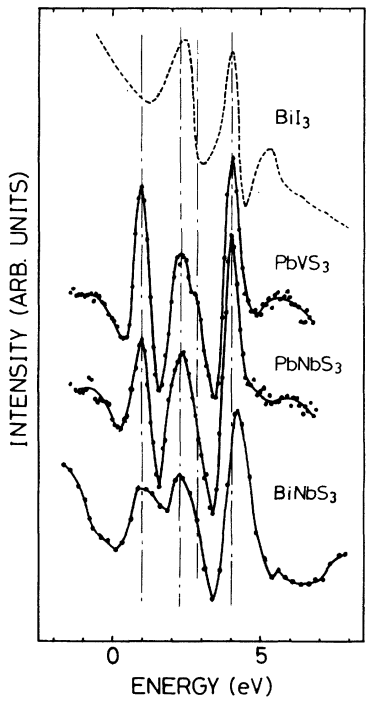

FIG. 14. Comparison of the Bi $O_{4,5}$ ISEELS spectrum in $BiNbS_3$ with the Pb $O_{4,5}$ ISEELS spectra in $PbVS_3$ and $PbNbS_3$ and the reflectivity spectrum in BiI_3 (Ref. 35).

D. Sn $N_{4,5}$ ISEELS spectra

1. Within the atomic model

Sn has an intermediate atomic number, i.e., 50, and the electronic configuration of the outermost shell is the same as that of Pb. The SO splitting of the outermost 5*p* levels is very small and the splitting of the inner-shell 4*d* levels is about 1.0 eV. Then we first try to explain the Sn $N_{4,5}$ ISEELS spectra in SnS and SnS_2 in terms of the multiplet structures in the *LS* coupling limit. For simplicity we assume that Sn in SnS and SnS_2 is localized as divalent and tetravalent ions, respectively. In this case the electronic configurations of the initial and final states are given by $4d^{10}4s^2$ ($^1S_0$), $4d^{10}$ ($^1S_0$), $4d^9 5s^2 5p^1$ ($^1F_3, ^1D_2, ^1P_1$), and $4d^9 5s^1$ ($^3D_1, ^3D_2, ^3D_3, ^1D_2$), respectively. Since the transition of the $^1S_1$ term to the $^1P_1$ term is optically allowed, we can observe a large peak for SnS even at large E_0. Since the transitions to the $^1F_3$, $^3D_1$, $^3D_2$, $^3D_3$, $^1D_2$ terms are optically forbidden, the oscillator strengths are small at $q=0$ and the higher-incident-energy ISEELS spectrum and the reflectivity spectrum exhibit only small structures at the threshold of SnS_2. As E_0 decreases, the intensities increase due to the breakdown of dipole selection rules. A large peak at 4 eV above the threshold is assigned to optically allowed transitions to the $4d^9 5p^1$ final state with the same multiplet terms as the $4d^9 5s^2 5p^1$ state. Figure 15 shows the Sn $N_{4,5}$ ISEELS spectra in SnS_2, SnS, and $SnTiS_3$. We may suggest from the comparison that the electronic configuration of Sn atoms in $SnTiS_3$ is close to that in SnS, although the appearance of structures around 30 eV shows a small deviation from it.

The absolute energy positions of the thresholds of these compounds agree within the experimental errors, although the XPS binding energies are different. A similar

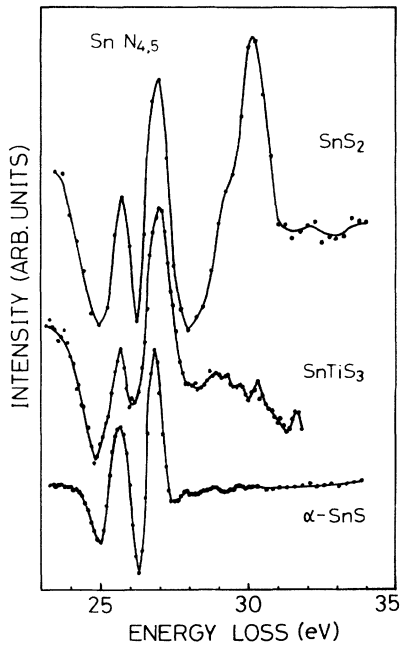

FIG. 15. Sn $N_{4,5}$ ISEELS spectra in SnS, SnS_2, and $SnTiS_3$.

result has been reported by van der Laan *et al.*[6] for Ni $L_{2,3}$ XAS spectra in the halides, which can be explained satisfactorily in terms of the atomiclike model involving interconfiguration interaction. The absolute energy position of the L_3 edge is almost unchanged, whereas the XPS binding energy is strongly compound dependent. In the study of Ref. 6, they have found that a core hole in XAS is effectively screened by an excited electron so that the probability of the shakeup process occurring is very small, whereas the poorly screened core-hole potential in XPS brings about the shakeup process; then the binding energies are different by the ligand ionization energy or the semiconducting energy gap. In the present case the difference is smaller than the semiconducting energy gap, and the oxidation number of Sn atoms is different between the compounds. Therefore the agreement might be accidental. Nevertheless it seems that the atomic model is valid for the Sn $N_{4,5}$ ISEELS spectra and the reflectivity spectra. The effects of j-j coupling may be neglected except for the splitting of the core levels and the reduced $I(N_5)/I(N_4)$ intensity ratio.

2. *Within the band-structure model*

Recently, Lefebvre *et al.*[38] have calculated the density of states (DOS) of several tin sulfides by an empirical tight-binding method. The calculated occupation number of 5s electrons is 1.9 and 1.2 for Sn with oxidation numbers II and IV in SnS and SnS_2, respectively. These electrons form a lone pair in SnS while in SnS_2 they participate in forming ionic-covalent bonds with surrounding S atoms. According to these band calculations, the conduction-band DOS of SnS is characterized by a large band consisting of Sn 5p states while the DOS of SnS_2 is characterized by two bands separated by 4 eV in the center of gravity; the lower-energy band is derived mainly from Sn 5s states and the higher-energy band is derived from Sn 5p states. Thus, we may expect that the transition from 4d levels to the bottom of the conduction band is optically allowed for SnS, but is forbidden for SnS_2. The first optically allowed transition for SnS_2 would occur at higher excitation energy, resulting in a large peak around 4 eV above the threshold. These results are confirmed by the experimental result described above. For SnS_2 the present author has shown in a previous paper[39] that there is a strong correlation between the Sn $N_{4,5}$ ISEELS spectrum and the S K XAS, the S $L_{2,3}$ ISEELS, and the bremsstrahlung isochromat spectra in which the core-hole interaction is small or not present. For SnS the energy distribution curve is compared with the S K XAS and the S $L_{2,3}$ ISEELS spectra in Fig. 16. We find that a similar correlation exists for these spectra. The smaller width of the first peak may be attributed to higher energy resolution of the Sn $N_{4,5}$ spectrum.

Cohen *et al.*[40] have recently indicated the presence of a core exciton in the Sn $N_{4,5}$ ISEELS spectrum in SnS_2. Monopole Coulomb interaction (F_0) causes a shift of spectral weight to lower energy. This attractive potential produces a uniform shift of structures in atomic spectra, but in a solid it breaks the translational symmetry, leading to variations in the DOS. If the interaction is large enough, a bound state called a core exciton appears below the conduction band. The main reason for their suggestion is the disagreement between the onset energy and the XPS binding energy of Sn $4d_{5/2}$ core levels with respect to the conduction-band minimum. However, the core-hole potential is screened less effectively in XPS [or ultraviolet photoelectron spectroscopy (UPS)] than in XAS, so that we must pay attention to whether the XPS (UPS) binding energy is used in deriving the energy of core levels in the ground state or not. Also, we must pay attention to the experimental result of Taniguchi *et al.*[41] that the sum of the band-gap energy and the Sn $4d_{5/2}$ UPS binding energy with respect to the top of the valence band gives the exact Sn N_5 onset energy for SnS and SnSe.

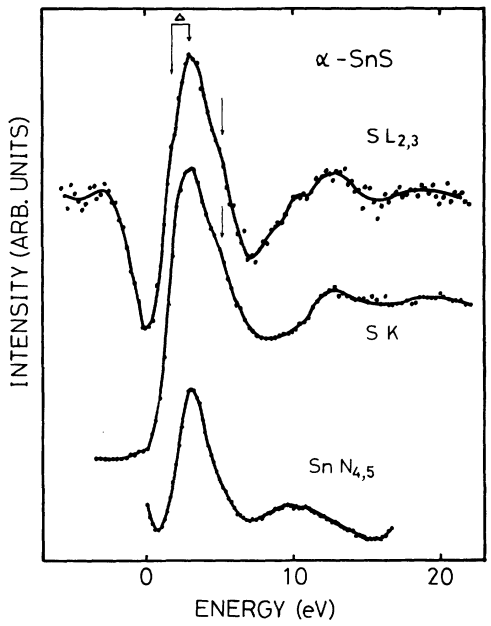

FIG. 16. Comparison of the low-resolution Sn $N_{4,5}$ ISEELS spectrum with S $L_{2,3}$ ISEELS and the S K XAS spectra for SnS. Δ denotes the spin-obit splitting of S 3p levels.

Another remaining problem is the reversed intensities of the N_5 and N_4 structures, which have been regarded as evidence of the e-h interaction.[41] If the conduction-band minimum consists mainly of $5p_{1/2}$-like states, we may explain the reversed intensities in terms of the matrix-element effect involving the spins, because the optically allowed $4d_{3/2} \rightarrow 5p_{1/2}$ transitions are predominant over the $4d_{5/2} \rightarrow 5p_{1/2}$ transitions, as discussed in Sec. III C. Unfortunately, there are no available band calculations involving the SO interaction of the outermost Sn 5p electrons at present.

IV. CONCLUSIONS

ISEELS spectra of a cation p or d hole in sulfides have been discussed, based on the atomic model and the energy-band-structure model. The shallow core holes interaction with valence electrons by an attractive Coulomb potential to a greater or lesser extent. If ex-

change and Coulomb interaction (*LS* coupling) is comparable to the SO splitting of the core levels, the spectra must be treated under intermediate-coupling conditions between the *LS* and *j-j* limits. Crystal-field interaction and interconfiguration interaction should be involved in the full atomic treatment. In the band-structure treatment, spins must be taken into account for the case that the SO splitting of the outermost unoccupied levels is not negligible, because the matrix elements are affected significantly by selection rules on the spin angular momentum. Optically allowed and forbidden transitions are distinguished by the incident-energy dependence, because dipole selection rules are broken at low E_0. Since $3d$ and $4d$ transition metals in layered TS_2 and MTS_3 compounds are bound strongly with surrounding S atoms, their ISEELS spectra are well explained in terms of the partial density of states. There is good agreement among the metal $M_{2,3}$ and $L_{2,3}$ and the S $L_{2,3}$ ISEELS spectra, the S K XAS spectrum, the IPS spectrum, and the calculated density of states for sulfides of the light $3d$ transition-metals. There is good agreement among the metal $M_{4,5}$ and $N_{2,3}$ and S $L_{2,3}$ ISEELS spectra, the metal L_3, S K and Se M_5 XAS spectra, the IPS spectrum, and the calculated density of states for the $4d$-transition-metal chalcogenides. The spectral variations due to donation of d electrons are consistent with those of the rigid-band model. The main features in the Pb and Bi $O_{4,5}$ ISEELS spectra are interpreted within the atomic model. The estimated SO splitting of the $5d$ levels is larger by 0.4 eV than the XPS value. Our estimated SO splittings of the $5d$ and $6p$ levels are 3.0 and 1.4 eV, respectively. The spectra reveal similar structures in spite of different crystal structures and different local atomic arrangements, arising from the optically forbidden $5d_{5/2} \rightarrow 6p_{1/2}$ transitions and the optically allowed $5d_{5/2} \rightarrow 6p_{3/2}$, $5d_{3/2} \rightarrow 6p_{1/2}$, and $5d_{3/2} \rightarrow 6p_{3/2}$ transitions. The first peak corresponding to the $5d_{5/2} \rightarrow 6p_{1/2}$ transitions disappears in the reflectivity spectra. The Sn $N_{4,5}$ ISEELS spectra in SnS and SnS_2 are roughly explained in terms of both the atomic model and the energy-band-structure model. Further discussion and experiments are necessary to answer the question as to which of them is more valid. It is also necessary to carry out band calculations involving spins, and full multiplet calculations under intermediate *LS* and *j-j* coupling conditions.

[1]S. Hüfner, in *Photoemission in Solids II,* edited by L. Ley and M. Cardona, Topics in Applied Physics Vol. 27 (Springer-Verlag, New York, 1979), p. 173.

[2]M. Campagna, G. K. Wertheim, and Y. Baer, in *Photoemission in Solids II,* Ref. 1, p. 217.

[3]B. T. Thole, G. van der Laan, J. C. Fuggle, G. A. Sawatzky, R. C. Karnatak, and J.-M. Esteva, Phys. Rev. B **32**, 5107 (1985).

[4]J. C. Fuggle, F. U. Hillebrecht, J. M. Esteva, R. C. Karnatak, O. Gunnarsson, and K. Schönhammer, Phys. Rev. B **27**, 4637 (1983).

[5]O. Gunnarsson and K. Schönhammer, Phys. Rev. B **28**, 4315 (1983).

[6]G. van der Laan, J. Zaanen, G. A. Sawatzky, R. Karnatak, and J.-M. Esteva, Phys. Rev. B **33**, 4253 (1986).

[7]J. Zaanen, G. A. Sawatzky, J. Fink, W. Speier, and J. C. Fuggle, Phys. Rev. B **32**, 4905 (1985).

[8]B. T. Thole and G. van der Laan, Phys. Rev. B **38**, 3158 (1988).

[9]L. Vriens, J. A. Simpson, and S. R. Mielczarek, Phys. Rev. **165**, 7 (1968).

[10]G. A. Wiegers and A. Meerschaut, J. Alloys Compounds **178**, 351 (1992).

[11]R. Lelieveld and D. J. W. Ijdo, Acta Crystallogr. B **34**, 3348 (1978); G. A. Wiegers, A. Meetsma, R. J. Haange, and J. L. de Boer, Acta Crystallogr. C **45**, 847 (1989).

[12]Y. Ohno, Phys. Rev. B **39**, 8209 (1989).

[13]Y. Ohno, Phys. Rev. B **36**, 7500 (1987).

[14]D. W. Bullet, J. Phys. C **11**, 4501 (1978).

[15]W. Drube, I. Schäfer, G. Karschnick, and M. Skibowski, Phys. Rev. B **30**, 6248 (1984).

[16]D. Straub, M. Skibowski, F. J. Himpsel, and W. Drube, Phys. Rev. B **31**, 8254 (1985).

[17]A. Zunger and A. J. Freeman, Phys. Rev. B **17**, 1839 (1978).

[18]R. D. Leapman, P. Rez, and D. F. Mayers, J. Chem. Phys. **72**, 1232 (1980).

[19]L. F. Mattheiss, Phys. Rev. B **8**, 3719 (1973).

[20]F. M. F. de Groot, J. C. Fuggle, B. T. Thole, and G. A. Sawatzky, Phys. Rev. B **41**, 928 (1980).

[21]T. Yamaguchi, S. Shibuya, S. Suga, and S. Shin, J. Phys. C **15**, 2641 (1982).

[22]Y. Gotoh, M. Goto, K. Kawaguchi, Y. Oosawa, and M. Onoda, Mater. Res. Bull. **25**, 307 (1990).

[23]F. M. F. de Groot, J. C. Fuggle, B. T. Thole, and G. A. Sawatzky, Phys. Rev. B **42**, 5459 (1990).

[24]A. R. Law and P. T. Andrews, Vacuum **41**, 553 (1990).

[25]G. A. Wiegers, A. Meetsma, R. J. Haange, and J. L. De Boer, J. Solid State Chem. **89**, 328 (1990).

[26]Y. Ohno, Phys. Rev. B **48**, 5515 (1993).

[27]B. Sonntag and F. C. Brown, Phys. Rev. B **10**, 2300 (1974).

[28]Y. Ohno, K. Hirama, S. Nakai, C. Sugiura, and S. Okada, Phys. Rev. B **27**, 3811 (1983).

[29]M. Sancrotti, L. Braicovich, C. Chemelli, and G. Trezzi, Solid State Commun. **66**, 593 (1988).

[30]M. Cardona, C. M. Penchina, E. E. Koch, and P. Y. Yu, Phys. Status Solidi B **53**, 327 (1972).

[31]G. Martinez, M. Schlüter, and M. L. Cohen, Phys. Rev. B **11**, 660 (1975).

[32]A. Santoni, G. Paolucci, G. Santoro, K. C. Prince, and N. E. Christensen, J. Phys. Condens. Matter **4**, 6759 (1992).

[33]F. R. McFeely, S. Kowalczyk, L. Ley, R. A. Poolak, and D. A. Shirley, Phys. Rev. B **7**, 5228 (1973).

[34]S. E. Kohn, P. Y. Yu, Y. Petroff, Y. R. Shen, Y. Tsang, and M. L. Cohen, Phys. Rev. B **8**, 1477 (1973).

[35]J. Bordas, J. Robertson, and A. Jakobsson, J. Phys. C **11**, 2607 (1978).

[36]S. P. Kowalczyk, L. Ley, F. R. McFeely, and D. A. Shirley, Solid State Commun. **17**, 463 (1975).

[37]G. Margaritondo and J. E. Rowe, Phys. Rev. B **19**, 3266 (1979).

[38]I. Lefebvre, M. Lannoo, J. O. Fourcade, and J. C. Jumas, Phys. Rev. B **44**, 1004 (1991).

[39]Y. Ohno, J. Phys. Soc. Jpn. **59**, 3740 (1990).

[40]H. Cohen, M. Folman, T. Maniv, R. Brener, E. Lifshiz, and Z. Esterlit, Phys. Rev. B **46**, 4446 (1992).

[41]M. Taniguchi, R. L. Johnson, J. Ghijsen, and M. Cardona, Phys. Rev. B **42**, 3634 (1990).